Taylor & Francis
Taylor & Francis Group

Atomic Dynamics and Diffusion in Decagonal Quasicrystals

F. GÄHLER and S. HOCKER

Institut für Theoretische und Angewandte Physik, Universität Stuttgart, D-70550 Stuttgart, Germany

The atomic dynamics of decagonal Al-Ni-Co and Al-Cu-Co quasicrystals is investigated by molecular dynamics simulations. Depending on the local environments, the mobility of the atoms varies greatly from site to site. Above two thirds of the melting temperature, a large fraction of the aluminium atoms become so mobile, that their diffusion can be measured directly in the simulation. As aluminium diffusion is hard to access experimentally, molecular dynamics simulations therefore provide a unique way to study aluminium diffusion in these complex systems.

Keywords Diffusion; molecular dynamics; quasicrystals

1. Introduction

Molecular dynamics (MD) simulations are clearly the tool of choice for the study of the *microscopic* dynamics in complex solids like quasicrystals. For a direct simulation of the resulting *macroscopic* effects, however, the accessible time scales are often too short. Atomic diffusion is such a slow process, which moreover is essential for the understanding of many physical processes in quasicrystals, including the formation of the equilibrium phase during high temperature annealing, and also the motion of dislocations and other defects. With the ever improving hardware and software technology, however, even slow processes may eventually become accessible to direct atomistic simulations. In this paper, we present MD simulations of decagonal quasicrystals, which show that at least the diffusion of aluminium is sufficiently fast to be directly measurable in the simulation. This is particularly fortunate, because aluminium diffusion is very hard to access experimentally, due to the lack of suitable radio-tracers [1]. Simulations can therefore replace the lacking experimental methods.

MD simulations over sufficiently long time scales are feasible only with classical effective potentials. Quantum-mechanical simulations would be limited to a few hundred atoms, which can neither provide enough statistics nor model the aperiodic nature of quasicrystals. We use for our simulations the Al-TM (transition metal) potentials of Moriarty and Widom [2, 3], which were derived from density functional theory and corrected by an additional empirical term [4]. These potentials, which we truncate smoothly at a radius of about 7.5 Å, have proved to work very well for these systems [3, 5]. A characteristic feature of the potential functions is their long range Friedel oscillations. All simulations were carried out with the code IMD [6] developed at our institute.
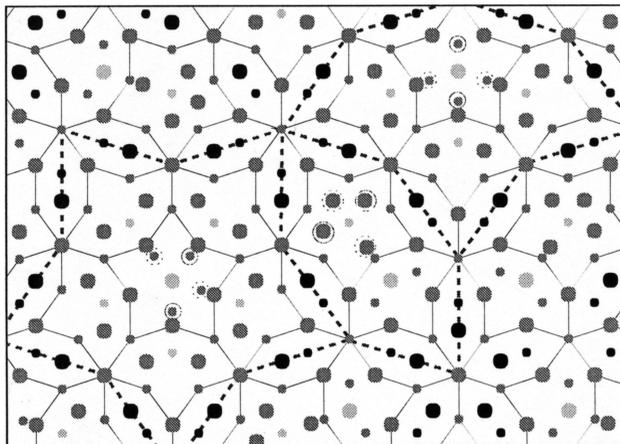
FIGURE 1 Ni-rich decoration after relaxation. The positions of the marked atoms differ from the original decoration [7]. Small (large) dots indicate atoms in upper (lower) layer. Al: dark grey, Ni: black, Co: light grey. Dashed lines mark supertiles containing three characteristic local neighbourhoods of star tiles. Encircled atoms occur only in every second double layer, those with solid circles in one half of the double layers, those with dashed circles in the other half.

2. Model Structures

We consider four different model structures, three for decagonal Al-Ni-Co, and one for decagonal Al-Cu-Co. All four models essentially consist of an alternating stacking of two different layers, which are decorations of the same hexagon-boat-star (HBS) tiling. This results in a periodicity of about 4 Å. All models share most of the atom positions; the difference lies mostly in the decoration of the TM sites. Apart from minor modifications [5], which break the 4 Å periodicity locally to an 8 Å periodicity, the first two decoration models for Al-Ni-Co have been derived in [7]. The first, so-called Ni-rich decoration ($Al_{70}Ni_{21}Co_9$) is shown in Fig. 1. The second decoration ($Al_{72}Ni_{17}Co_{11}$) is derived from it by replacing certain Ni-Ni pairs in hexagon supertiles by Co-Al pairs, which has turned out to be energetically favourable [7]. This decoration is called Co-rich, although its composition is still in the Ni-rich corner of the existence domain. The third decoration ($Al_{72}Ni_{20}Co_8$) is inspired by the cluster model of Abe et al. [8], and therefore called the Abe decoration. To a large extent, its Ni-Co decoration is reversed with respect to the Ni-rich decoration. The supertiles contain Co instead of Ni, and the Ni-Ni pairs on supertile edges are replaced by Ni-Co pairs, or a TM-vacancy pair [8]. The Ni-Co decoration of the Abe model is not supported by total energy calculations [7, 9], but serves for an interesting comparison. Finally, for decagonal Al-Cu-Co we use a variant [10] of the decoration proposed by Cockayne et al. [11], with a composition of $Al_{70}Cu_{10}Co_{20}$. It is obtained from the Ni-rich decoration by replacing each Ni-Ni pair on supertile edges by a Cu-Co pair. If the supertile edge points to an acute corner of a tile, the Cu atom is always placed close to that corner.

3. Atomic Dynamics

As a first test of the potentials, the melting temperature T_m was determined by slow heating at constant pressure. All samples melted within 5–10% of the experimental melting temperature of about 1200 K [12]. The remaining simulations were carried out at constant
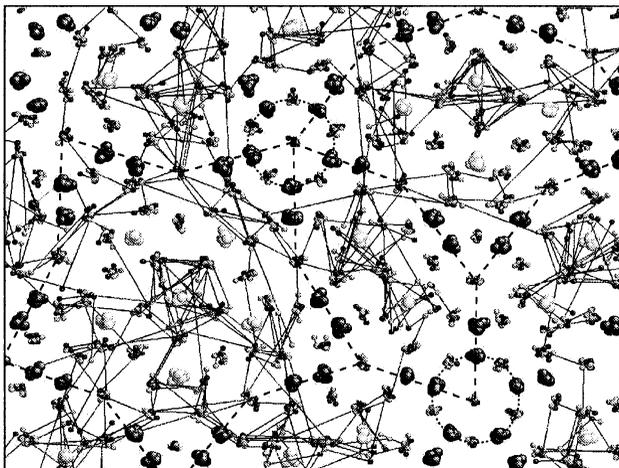
FIGURE 2 Al motion at $T = 0.9T_m$ in the Ni-rich sample. Dark grey, large: Ni; light grey, large: Co; dark grey, small: Al initial positions; light grey, small: Al positions after 100ps. Initial and final Al positions are connected. Supertiles and stable clusters are marked.

temperature and volume, where the pressure was first adjusted by scaling the sample. Apart from initial relaxations, all samples remained essentially stable up to the melting temperature. Nevertheless, above 0.6 T_m significant Al diffusion is observed (Fig. 2), which does not destroy the overall structure, however. This can be seen in time-averaged atom density maps (Fig. 3), which show that all TM sites and some Al sites remain very sharp over a 2ns simulation period, whereas most of the other Al sites are smeared out in certain directions, but still stable and well identifiable. The most mobile Al atoms are the ones near the Co sites of the Ni-rich decoration. A comparison with the other samples shows that this mobility is not so much due to the Co atoms, but rather due to the geometric environment of the Co sites. In the Abe model, where the corresponding sites are occupied by Ni, the same Al atoms show the enhanced mobility. The mobile Al atoms also quickly
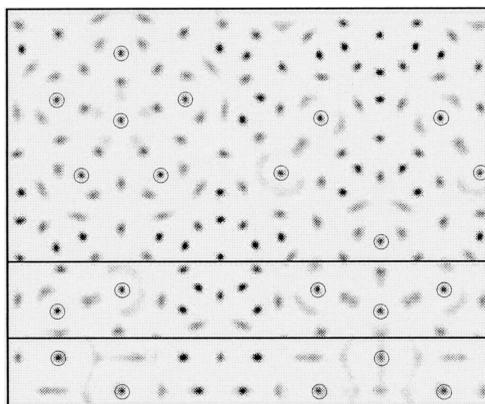
FIGURE 3 Atom density map of Ni-rich Al-Ni-Co, averaged over 2ns. In the top and middle parts, the projection on the *xy* plane is shown. The bottom part shows the strip in the middle, projected on the *xz*-plane. Co is marked with circles; Ni appears as sharp, almost black dots, whereas Al positions are grayish.
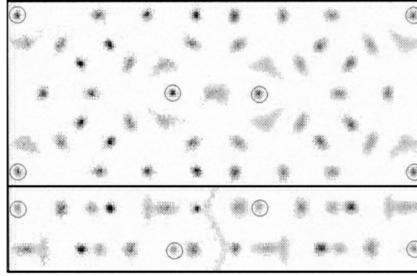
FIGURE 4 Atom density distribution for classical MD (left half) and ab-initio MD (right half), for a small sample of one supertile hexagon. Shown is the projection on the *xy*-plane (top) and on the *xz*-plane (bottom). Co is marked with circles; Ni appears as sharp, almost black dots, whereas Al positions are grayish.

absorb the vacancies initially present in the Abe model. Only 75–80% of the Al atoms show a high mobility. Others remain stable, notably those in fivefold Al-Ni clusters (see Figs. 2 and 3). The mobile Al atoms are sufficiently frequent to make long range diffusion possible.

The atom density maps (Fig. 3) reveal that the banana shaped Al sites inside supertile hexagons are smeared out only horizontally, whereas the central dot in the hexagon is actually a zig-zag shaped distribution continuous along the z-axis (compare also [9]). In fact, the potential valleys of the Al atoms are shallow only along one direction, but enhanced Al mobility can occur in all directions. The smeared-out Al sites certainly have to be taken into account in the interpretation of diffraction data, and possibly can explain some of the diffuse scattering that is intrinsic in these quasicrystals [13].

To corroborate the correctness of the potentials, we have simulated a small sample of just four supertile hexagons (100 atoms) both with ab-initio MD and with classical MD, under precisely the same conditions. The ab-initio simulations, which were carried out with the VASP code [14], could span a time interval of only 20 ps, so that it is not possible to measure diffusion directly. However, the atom density maps obtained in these simulations are remarkably similar (Fig. 4). In particular, all Al sites are smeared out in exactly the same way.
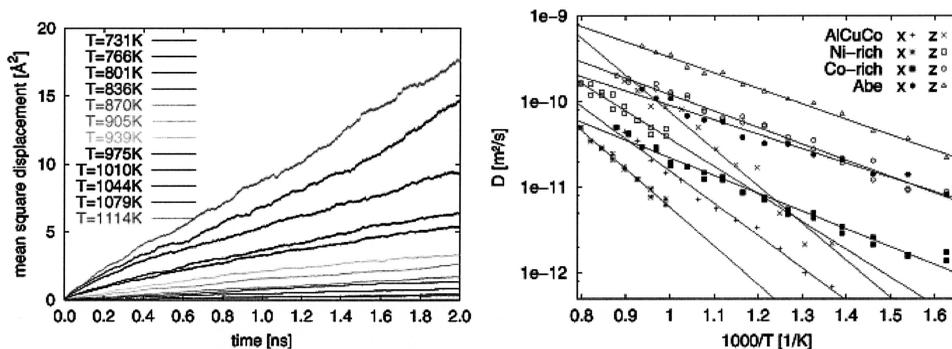
FIGURE 5 Mean square displacement of Al in *x*-direction for Al-Cu-Co, at different temperatures (left). Arrhenius plots for Al diffusion (right).

TABLE 1 Activation Enthalpies and Pre-exponential Factors for Al Diffusion

Sample		Ni-rich	Co-rich	Abe	Al-Cu-Co
ΔH_{xy}	$[eV]$	0.89	0.41	0.34	0.75
ΔH_z	$[eV]$	0.64	0.38	0.35	0.86
D_{0xy}	$[m^2/s]$	$1.8\,10^{-7}$	$2.6\,10^{-9}$	$4.6\,10^{-9}$	$9.0\,10^{-8}$
D_{0z}	$[m^2/s]$	$6.3\,10^{-8}$	$9.7\,10^{-9}$	$1.8\,10^{-8}$	$1.5\,10^{-6}$

4. Aluminium Diffusion

To determine the diffusion of Al quantitatively, the mean square displacement (MSQD) of Al is measured as a function of time for many temperatures. As illustration, some of the MSQD curves for the Al-Cu-Co sample are shown in Fig. 5 (left). Similar curves for the Ni-rich sample have been published in [5]. From the slope of these curves, the diffusion constant is easily extracted, and can be fitted to the usual Arrhenius law for the diffusion constant D,

$$D = D_0 e^{-\Delta H/k_B T} \tag{1}$$

from which the activation enthalpy ΔH and pre-exponential factor D_0 can be determined, separately for the x-, the y-, and the z-directions. The numerical values are given in Table 1, and the fit to the Arrhenius law is shown in Fig. 5 (right). The diffusion is slightly anisotropic, by a factor 2–3 faster in the periodic direction. The activation enthalpies are rather small, compared with the value for vacancy-mediated diffusion in FCC Al (1.3 eV) [15]. However, one must keep in mind that due to the short simulation time, diffusion vehicles like vacancies may not be in thermal equilibrium, so that only their migration enthalpy is measured [16]. On the other hand, except for the Abe model our samples did not contain any vacancies, so that the diffusion we observe must be due to a different mechanism. For non-Al diffusors, Mehrer and Galler [17] have concluded that a vacancy mechanism is dominant. For Al diffusion, the role of vacancies remains unclear.

5. Discussion and Conclusion

Our simulations have shown that MD simulations are suitable to determine aluminium diffusion in quasicrystals quantitatively, which is not possible by experiment. The correctness of these results crucially depends on the quality of the potentials, which so far have been tested mainly for ground state type structures [3], not at temperatures close to the melting point. It is unclear whether the energetics of the diffusion processes at high temperatures are described completely correctly, so that there is some uncertainty in the numerical values given in Table 1. However, the diffusion of Zn in decagonal Al-Ni-Co, which is believed to be similar to Al, is of the same order [18] when extrapolated to the high temperatures considered here. Also the comparison with ab-initio simulations (Fig. 4) adds confidence to our results.

Our simulations could not confirm the experimental evidence for vacancy-mediated diffusion [17]. Vacancies initially present in the Abe model have even been dissolved. It may be that a proper simulation of systems with vacancies would require many-body potentials, like EAM potentials [19]. Simple pair potentials are well known for not being able to describe vacancies adequately. Unfortunately, EAM potentials are presently not available for such complicated structures.

References

1. H. Mehrer, R. Galler, W. Frank, R. Blüher, and A. Strom, in *Quasicrystals: Structure and Physical Properties*, ed. H.-R. Trebin, Wiley-VCH 2003, p. 312.
2. J. A. Moriarty and M. Widom, *Phys. Rev. B* **56**, 7905 (1997).
3. M. Widom, I. Al-Lehyani, and J. A. Moriarty, *Phys. Rev. B* **62**, 3648 (2000).
4. I. Al-Leyiani et al., *Phys. Rev. B* **64**, 075109 (2001).
5. F. Gähler and S. Hocker, *J. Non-Cryst. Solids* **334–335**, 308 (2004).
6. J. Stadler, R. Mikulla, and H.-R. Trebin, *Int. J. Mod. Phys. C* **8**, 1131 (1997). http://www.itap.physik.uni-stuttgart.de/˜imd/
7. M. Mihalkovič et al., *Phys. Rev. B* **65**, 104205 (2001).
8. E. Abe et al., *Phys. Rev. Lett.* **84**, 4609 (2000).
9. C. L. Henley, M. Mihalkovič, and M. Widom, *J. All. Comp.* **342**, 221 (2002).
10. I. Al-Lehyani and M. Widom, *Phys. Rev. B* **67**, 014204 (2003).
11. E. Cockayne and M. Widom, *Phys. Rev. Lett.* **81**, 598 (1998).
12. S. Ritsch et al., *Phil. Mag. Lett.* **78**, 67 (1998).
13. F. Frey and E. Weidner *Z. Kristallogr.* **218**, 160 (2003).
14. http://cms.mpi.univie.ac.at/vasp/
15. S. Dais, R. Messer, and A. Seeger, *Mat. Sci. Forum* **15–18**, 419 (1987).
16. S. Grabowski, K. Kadau, and P. Entel, *Phase Trans.* **75**, 265 (2002).
17. H. Mehrer and R. Galler, *J. All. Comp.* **342**, 296 (2002).
18. G. Kresse and D. Joubert, *Phys. Rev. B* **59**, 1758 (1999).
19. M. S. Daw and M. T. Baskes, *Phys. Rev. B* **29**, 6443 (1984).